Case Studies in Thermal Engineering 53 (2024) 103931

Contents lists available at ScienceDirect

Case Studies in Thermal Engineering

journal homepage: www.elsevier.com/locate/csite

Potential coolants for fuel cell application: Multi-objective optimization of thermophysical properties and PPF calculation of hybrid palm oil nanofluids

A.G.N. Sofiah [a,*], J. Pasupuleti [a,**], M. Samykano [b], R. Kumar Rajamony [a,c], A.K. Pandey [d,e], Nur Fatin Sulaiman [f], Zatil Amali Che Ramli [a], S.K. Tiong [a], S.P. Koh [a]

[a] Institute of Sustainable Energy, Universiti Tenaga Nasional (The Energy University), Jalan Ikram-Uniten, Kajang, 43000, Selangor, Malaysia
[b] Centre for Research in Advanced Fluid and Processes, Universiti Malaysia Pahang Al-Sultan Abdullah, 26300, Gambang, Pahang, Malaysia
[c] Division of Research and Development, Lovely Professional University, Phagwara, Punjab, 144411, India
[d] Research Centre for Nano-Materials and Energy Technology (RCNMET), School of Science and Technology, Sunway University, No. 5, Jalan Universiti, Bandar Sunway, Petaling Jaya, 47500, Selangor Darul Ehsan, Malaysia
[e] Center for Transdiciplinary Research (CFTR), Saveetha University, Chennai, India
[f] Institute of Informatics and Computing in Energy, Universiti Tenaga Nasional (The Energy University), Jalan Ikram-Uniten, Kajang, 43000, Selangor, Malaysia

ARTICLE INFO

Handling Editor: Huihe Qiu

Keywords:
Hybrid nanofluid
Density
Viscosity
Thermal conductivity
Energy
RSM
PPF

ABSTRACT

In this study, Response Surface Methodology (RSM) is being used to optimize density, viscosity, and thermal conductivity in CuO-polyaniline/palm oil hybrid nanofluids. Using a Central Composite Design (CCD) within RSM, researchers are systematically exploring the impact of temperature (ranging from 30 to 60 °C), volume concentration of nanoadditives (varying from 0.1 to 0.5 vol%) and CuO composition (ranging from 1 to 10 wt%) on the thermophysical properties of these nanofluids. This research is pioneering in its evaluation of the price performance factor (PPF) for these nanofluids. To ensure model reliability, Analysis of Variance (ANOVA) is being applied. The findings showcase robust models, as indicated by a 45° angle line within the predicted vs. actual data graph. The models exhibit impressive R^2 values: 98.66 % for density, 99.93 % for viscosity, and 99.91 % for thermal conductivity, underscoring the agreement between predicted and actual data. Optimal values for density, viscosity, and thermal conductivity are being obtained: 0.901532 g/mL, 37.1229 mPa s, and 0.356891 W/mK, respectively. These correspond to critical parameters of 53.92 °C for temperature, 0.038 vol% for volume concentration of nanoadditives and 2.90 wt% for CuO composition. Moreover, the price performance factor (PPF) assessment reveals that higher thermal conductivity doesn't necessarily equate to greater cost-effectiveness.

1. Introduction

Recently, the development in automotive system is confronted with significant challenges related to the reduction of greenhouse gas emissions and the maintenance of energy security, particularly as low-cost petroleum resources become scarcer [1,2]. The

* Corresponding author.
** Corresponding author.
E-mail addresses: nurhanis.sofiah@uniten.edu.my, nurhanisofiah@gmail.com (A.G.N. Sofiah), jagadeesh@uniten.edu.my (J. Pasupuleti).

https://doi.org/10.1016/j.csite.2023.103931
Received 9 October 2023; Received in revised form 12 December 2023; Accepted 17 December 2023
Available online 20 December 2023

escalating demand for energy in conjunction with concerns about environmental pollution and the depletion of fossil fuels has intensified the exploration of fuel cell technology as a feasible alternative to fossil fuel-based energy systems [3]. Projections indicate that fuel cell electric vehicles could yield the most substantial reductions in emissions and petroleum-derived fuel usage among advanced vehicle options by the year 2050 [4,5]. Particularly, fuel cell technology have demonstrated considerable potential as energy conversion systems in automotive applications. Noteworthy advantages of these cells encompass their high power density, rapid startup capabilities, relatively low operational temperatures, elevated efficiency in converting electrical energy, compact dimensions, low weight, extended lifespan, and the ability to function effectively during stop-start driving conditions [6,7].

The thermal management system of fuel cell devices is essential to ensure the efficient operation of the devices. The thermal management system of a fuel cell involves controlling the operating temperature within an optimum range to ensure that heat energy is distributed evenly across the stacks and membranes [8]. Cooling systems for fuel cells commonly utilize either a liquid or air to move through cooling channels within bipolar plates or cooling plates. Liquid cooling becomes necessary for fuel cells with a power output of 10 kW or more, whereas air cooling alone suffices for fuel cells up to 2 kW. Within this range, careful choices must be made regarding whether to opt for liquid or air cooling methods [9,10].

The commercially used approach to enhance the cooling rate involves either increasing the thermal removal area or boosting the flow rate of the coolant. However, these methods result in an unwanted enlargement of the components within thermal management systems [11,12]. Simultaneously, the poor inherent thermo physical behavior of conventional heat transfer fluids like water, ethylene glycol, or oil significantly curtail cooling efficiency. Over the past few decades, researchers have endeavored to create fluids that offer superior in ability to transfer heat energy for various thermal systems when compared to conventional heat transfer fluids [13,14]. Specifically, for fuel cell applications, the U.S. Department of Energy has undertaken multiple projects focused on developing coolant solutions with prolonged durability, high thermal conductivity, and minimal electrical conductivity for the operation of proton exchange membrane fuel cells [15,16]. These efforts aim to enhance the overall performance and resilience of fuel cell devices.

Additionally, in fuel cell devices, the produced electrical energy generates the electrical field that may affects the polarization of the coolants and as a consequent, may cause the electricity leaks via the channel of the coolants [17,18]. Palm oil, due to its inherent low electrical conductivity properties, holds promising potential for utilization as a coolant within fuel cell systems [19]. The thermal conductivity properties of palm oil can be enhanced through the introduction of nanoparticles into its composition to form a nano enhanced heat transfer fluids. A technologically sophisticated heat transfer fluid known as a nanofluid is created by incorporating nanoparticles into base fluids [20,21]. This innovation has garnered significant interest among researchers owing to its exceptional heat transfer capabilities. The electrical conductivity of the coolants can either maximize or minimize corresponding to the properties of membrane, dimension of nanoparticles and volume concentration of nanoparticles. Nonetheless, for the nanofluids to be serve as coolant for fuel cell devices, it is beneficial to enhance the thermal conductivity properties, without enhancing the electrical conductivity behavior of the coolants. Hitting these both requirements may be a very crucial task [22,23].

Pourfayaz et al. [24] conducted a study on an integrated polymer electrolyte membrane fuel cell paired with an absorption chiller. This chiller employed various nanofluids—aluminum nanoparticles-water nanofluid, silver nanoparticles-water nanofluid, and aluminum oxide nanoparticles-water nanofluid—as refrigerants, with the goal of enhancing the coefficient of performance of the integrated system. The study found that the refrigerant containing silver nanoparticles dispersion achieved an overall efficiency of 81 %. In another investigation, Kordi et al. [25] employed a numerical approach to explore the performance of a polymer electrolyte membrane fuel cell assisted by aluminum oxide nanoparticles-water nanofluid as a cooling agent. Different volume concentrations of aluminum oxide nanoparticles were dispersed in the base fluid to analyze the effect of nanoadditive volume concentration on the cooling rate of a four-plate cooler. The numerical study revealed that the application of nanofluid improved the cooling rate and notably boosted the fuel cell's efficiency. Specifically, a nanofluid with a volume concentration of 0.006 % resulted in a 13 % decrease in the temperature uniformity index, while causing a 35 % increase in pressure drop. This suggests that nanofluids can enhance the heat transfer behavior of cooling plate devices, ultimately leading to improved fuel cell performance.

More recently, Khani et al. [26] conducted an experimental investigation on the heat transfer performance of water-based nanofluids with different nanoadditives (α-alumina nanoparticles, α-alumina nanoparticles with copper oxide nanoparticles, and α-alumina nanoparticles with iron oxide nanoparticles). These nanofluids were considered as potential coolants for polymer electrolyte membrane fuel cell systems. Various weight percentages of nanoadditives and sodium dodecyl sulfate surfactant were dispersed to assess their impact on the heat transfer behavior of the formulated nanofluids. The study reported a substantial 21.4 % enhancement in the thermal performance of 0.3 wt% modified surface α-alumina nanoparticles-water nanofluids with an adequate amount of surfactant. This noteworthy improvement in the heat transfer properties of the formulated nanofluids indicates their suitability as effective coolants for fuel cell devices, contributing to the overall system's higher efficiency.

Due to their limited thermophysical behavior, a nanocoolant with higher thermal conductivity properties but lower in viscosity and density is required to improve the cooling rates in thermal management system and thus, enhance the performance of the fuel cell devices. Hence, the current study seeks to examine the density, viscosity and thermal conductivity of palm oil combined with cost-effective and environmentally friendly polyaniline nanofibers and copper oxide nanoparticles as a potential heat transfer medium. Basically conductive polyaniline nanofibers may exists in two forms, namely non-doped conducting polyaniline and doped-conductive polyaniline nanofibers. The phenomenon to convert non-conductive state of polymers backbone into π – conjugated charged conductive chains is usually termed as "doping". The properties of a polyaniline nanofibers changes comprehensively by doping the neutral form of polymer with a small amount of dopant materials (≈10 wt%) [27,28]. The selection of the 1–10 wt% range for doping polyaniline with copper oxide nanoparticles was chosen as it represents a balanced approach to achieve the desired enhancement in properties. This range is within the typical limits suggested in the literature, and it allows for effective doping without potential negative consequences associated with excessive doping.

The resulting heat transfer fluid is subsequently analyzed to assess the impact of applied temperature, volume concentration of nanoadditives and various composition parameters on its attributes. To the best of authors knowledge, no prior investigation has delved into the application of Response Surface Methodology (RSM) for modeling and optimizing hybrid copper oxide-polyaniline nanocomposites dispersions within palm oil base fluids. This current study aims to formulate a multifaceted empirical correlation using RSM, encompassing numerous input parameters like volume concentration of nanoparticles and temperature. This inclusive employment of multiple input parameters ensures the precise prediction of nanofluid density, viscosity and thermal conductivity and permits experimental scrutiny of the viscous behavior inherent to nanofluids composed of copper oxide-polyaniline nanocomposites. Furthermore, the model devised will be applied to ascertain the optimal input parameters for either minimizing or maximizing of these studied properties. The price performance factor is also calculate in order to investigate the economic status of the studied nanofluids as formulated parameters.

2. Methodology

2.1. Materials and resources

The synthesis of nanoadditives, formulation of nanofluids, physical characterization of nanoadditives, stability examination, and measurements of thermal physical properties are derived from earlier research study [29].

2.2. Response Surface Methodology

The response surface methodology (RSM) is used to develop a mathematical equation from the obtained experimental data. The RSM can generate the optimal parameter value based on the mathematical and statistical technique. The effect of temperature factor and volume concentration factor on specific responses of density, viscosity, and thermal conductivity (as presented in Table 1) was estimated via central composite design (CCD). The calculation of a full quadratic mathematical regression model was generated via Design Expert 7.1.6 software by examining the regression coefficient, analysis of variance (ANOVA), and diagnostic of the model graphs. The fit quality of the developed mathematical equation model was analyzed to investigate the developed model's reliability. The basic mathematical equation model in RSM is based on a linear function and is presented in Equation 1 [30,31].

$$Y = \boldsymbol{\beta}_{o} + \sum_{i=1}^{n} \beta_i x_i{}^1 + \sum_{i=1}^{n} \beta_{ii} x_i{}^2 + \sum_{i=1}^{n} \beta_{ij} x_i + \varepsilon^1 \tag{1}$$

where, Y is the predicted response, n is the number of variables, $\boldsymbol{\beta}_0$ is the intercept, $\boldsymbol{\beta}_i$ represents the first model of linear parameters, $\boldsymbol{\beta ii}$ the second-order (quadratic) coefficient, $\boldsymbol{\beta ij}$ the coefficient of an interaction effect, x_i and x_j represents variables and ε is the residual associated to the experiments, and the second-order model This model may cover a variety of functions.

The relationship between continuous variables and response variables is expressed in a mathematical regression equation. A systematic comparison was conducted between the experimental and prediction data and the results obtained from the regression comparison in order to determine the validity of the generated regression model. The influence of temperature, volume concentration and CuO composition on density, viscosity and thermal conductivity properties is studied for about 20 runs. Table 2 summarizes the layout design with the findings from the experimental data.

2.3. Price performance factor evaluation

The economic analysis was evaluated by using price performance factor (PPF) equation [32–34] as presented in Equation (2):

$$PPF = \frac{RTC}{price\left(\frac{\$}{liter}\right)} \tag{2}$$

The obtained data from thermal conductivity measurement were further used for relative thermal conductivity calculation as summarized in Table S2 (supplementary information). The PPF was analyzed by calculating the cost of formulation each liter of CuO-polyaniline/palm oil nanofluids at different volume concentration of polyaniline nanofibers (0.1–0.5 vol%), and different composition of copper oxide nanoparticles (1–10 wt%) at temperature of 30 °C, 40 °C, 50 °C 60 °C. The preparation expenses of the studied nanofluids was tabulated in Table S1 (supplementary information).

3. Results and discussion

RSM was utilized to establish an empirical connection between the input variable and the corresponding response. Following the formulation of the equation, an analysis of variance (ANOVA) was applied to optimize the response. The model's significance and its

Table 1
Levels of factors.

Type of Factors	Factors	−1	+1
Continuous factors	Temperature (°C)	30	60
	Volume concentration (vol%)	0.1	0.5
	Amount of CuO nanoparticles (wt%)	1	10

Table 2
Design of experiments and its findings.

Std	Temperature (°C) Factor A	Volume Concentration (vol%) Factor B	CuO composition (wt%) Factor C	Density (g/ml)	Viscosity (mPa.s)	Thermal Conductivity (W/mK)
1	60	0.3	5	0.8999	28.613	0.3835
2	40	0.3	5	0.9054	57.994	0.2778
3	40	0.3	5	0.9061	58.001	0.279
4	30	0.5	1	0.90976	76.236	0.2398
5	50	0.1	10	0.90289	42.901	0.3031
6	50	0.1	1	0.90216	40.834	0.3089
7	40	0.3	5	0.9044	57.811	0.2801
8	50	0.5	10	0.90405	45.893	0.338
9	40	0.5	5	0.90658	58.298	0.2888
10	50	0.5	1	0.90315	44.354	0.3437
11	60	0.3	5	0.8999	28.613	0.3835
12	40	0.3	1	0.90523	57.804	0.279
13	30	0.3	5	0.90911	76.131	0.2301
14	30	0.1	1	0.90886	75.472	0.2296
15	40	0.3	10	0.9066	59.021	0.2745
16	40	0.3	5	0.906	57.799	0.2803
17	40	0.3	5	0.9051	58.021	0.2766
18	30	0.5	10	0.91069	79.492	0.2346
19	40	0.1	5	0.90464	57.761	0.2645
20	30	0.1	10	0.90952	76.681	0.2174

parameters were assessed using ANOVA for the quadratic polynomial. The ANOVA analysis generated the mean square for each input, the sum of squared deviations, and the degree of freedom for the model. An input is considered significant if either its numerical value or the model's p-value corresponding to the F value is less than 0.05, as per the 95 % confidence interval in RSM. The developed model serves to elucidate the relationships between the parameters (A, B, and C), the interactions among parameters (AB, AC, and BC), and the squares of inputs (A^2, B^2, C^2) [35,36].

3.1. *Influence of independent variables on density of copper oxide-polyaniline/palm oil hybrid nanofluids*

The purpose of regression study is to check the best-fitted regression from the obtained experimental data in the form of mathematical regression model as proposed in Equation (3). Table 3 summarized informative contribution of every single generated term in the developed mathematical model. F-values and P-values represents the ability of the proposed model and separation values of relevant and irrelevant relationship boundaries respectively. Less than 0.05 of P-value reflects as an essential correlation parameters while more than 0.1 P-value indicate that the parameters has no significant impact. The table indicates that the F-value for the developed model is 81.87, with a corresponding P-value of less than 0.05. According to the main model, terms A, B and C were shown to have a considerable impact on density of nanofluids. These findings show that the proposed model is significant. ANOVA generates the assurance of R^2 and standard deviation which represent the reliability of the proposed equation. 0.9866 and 4.90E-04 of R^2 and standard deviation values respectively verify that 98.66 % of the total variation can be correspondent by the proposed regression equation. Besides, the 96.75 % and 97.46 % of predicted R^2 and adjusted R^2 respectively indicate the reliable agreement.

Table 3
The density's empirical model results using ANOVA.

Parameter	Sum of square	Degree of freedom	Mean Squares	F value	P-value	
Model	1.77E-04	9	1.96E-05	81.87	<0.0001	significant
A-Temperature	1.40E-04	1	1.40E-04	583.28	<0.0001	
B-Volume Concentration	2.95E-06	1	2.95E-06	12.29	0.0057	
C–CuO composition	1.63E-06	1	1.63E-06	6.79	0.0262	
AB	8.00E-10	1	8.00E-10	3.34E-03	0.9551	
AC	3.23E-10	1	3.23E-10	1.35E-03	0.9714	
BC	1.63E-08	1	1.63E-08	0.068	0.7997	
A^2	1.44E-06	1	1.44E-06	6.01	0.0342	
B^2	1.13E-07	1	1.13E-07	0.47	0.5086	
C^2	6.19E-07	1	6.19E-07	2.58	0.1392	
Residual	2.40E-06	10	2.40E-07			
Lack of Fit	4.58E-07	5	9.15E-08	0.24	0.9306	not significant
Pure Error	1.94E-06	5	3.88E-07			
Correlation Total	1.79E-04	19				
Standard Deviation	4.90E-04	R-Squared	0.9866			
Mean	0.91	Adj R-Squared	0.9746			
C.V. %	0.054	Pred R-Squared	0.9675			
PRESS	5.82E-06	Adeq Precision	31.538			

$$Density = 0.92 - 5.68E\text{-}004*A - 2.17E\text{-}004*B - 1.62E\text{-}004*C + 5E\text{-}006*A*B + 1.41E\text{-}007*A*C + 5E\text{-}005*B*C + 2.91E\text{-}006*A^2 + 4.71E\text{-}003*B^2 + 2.21E\text{-}005*C^2 \quad (3)$$

Fig. 1(a) presents normal plot of residual for density of CuO-polyaniline/palm oil hybrid nanofluids data. The generated graph displays all data plotted within one straight line, validating that the value of residual is having appropriate standard error terms. An effective model point should exhibit no discernible pattern, with values closely aligning with a straight line. The normal plot of residuals clearly demonstrates that the data points do not adhere to any specific trend and instead cluster near the straight line, confirming a random distribution. To further mitigate deviations in the data points, an outlier plot is essential, as depicted in Fig. 1(b). Data points falling outside the acceptable range (±3.0) are considered unreliable. Notably, Fig. 1(b) illustrates that all data points remain within the permissible range.

The final step involves the validation of the developed model using experimental data. The comparison of estimated density by developed mathematical model with the present experimental data is revealed in Fig. 2. The formation of 45° angle line in the middle of the graph that align with all the plotted data showing an excellent agreement of both predicted and actual data and verified the reliability of the generated regression equation for response prediction.

Fig. 3 shows the contour plot and 3D surface plot for the developed model. The contour plot and 3D surface plot is plotted to study the interaction of nanofluid concentration, temperature and CuO composition to the density of nanofluids. The contour plot for density versus volume concentration, temperature and CuO composition is shown in Fig. 3(a–c). The plot shows that higher concentrations of nanoadditives in the palm oil lead to higher densities, while lower temperatures also lead to higher densities. At the same time, based on the contour plot analysis, the CuO composition does not significantly impact the density as compared to the other input variables (nanofluid concentration and temperature). Based on the 3D surface plot analysis in Fig. 3(d–f), the CuO composition does not significantly impact the density of CuO-polyaniline/palm oil nanofluids compared to the other input variables (volume concentration and temperature). This means that changes in CuO composition do not cause significant changes in the density of the nanofluid. In contrast, changes in the volume concentration of nanofluids and the temperature at which it is tested have a much greater impact. It is evident from the contour plot analysis in Fig. 3(d) that higher density of nanofluid obtained with increasing of volume concentration at lower temperature. This means that when the nanoadditives amount increases, the density increases because the solid-state material's density inside the nanoadditives is higher than liquid. The reduction in density for all nanofluids was significantly different with the temperature change due to the bonds in base fluids break more slowly as temperature decreases and the structure tend to trap fewer extra liquid molecules [37–40]. Overall, the contour plot and 3D surface plot suggests that controlling the concentration of nanoparticles and the temperature at which the fluid is tested are important factors in determining the density of nanofluids.

3.2. *Influence of independent variables on viscosity of copper oxide -polyaniline/palm oil hybrid nanofluids*

Table 4provides a concise summary of the informative contributions made by each individual term within the developed mathematical model in Equation (4). The table highlights that the F-value for the developed model is 1550.05, accompanied by a corresponding P-value of less than 0.05. These results affirm the significance of the proposed model. According to the main model, terms A, B and C were shown to have a considerable impact on viscosity of nanofluids. Additionally, the ANOVA provides assurance regarding R^2 (coefficient of determination) and standard deviation, which reflect the reliability of the proposed equation. Values of 0.0.9993 for R^2 and 0.56 for standard deviation indicate that the proposed regression equation can account for 99.93 % of the total variation. Furthermore, predicted R^2 and adjusted R^2 values of 99.23 % and 99.86 %, respectively, demonstrate a high level of reliable agreement.

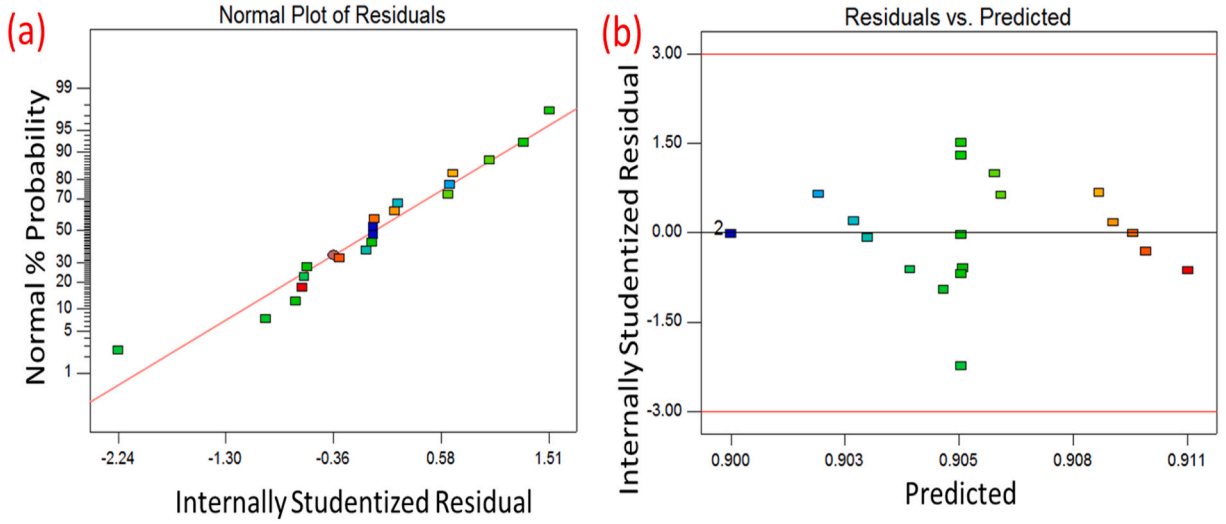

Fig. 1. Model's adequacy tests for density; (a) Normal residual plot, (b) Outlier plot.

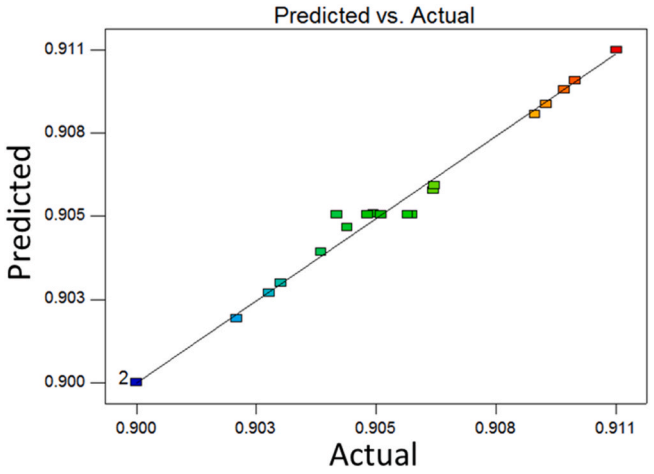

Fig. 2. Predicted vs. actual plot on density of CuO-polyaniline/palm oil hybrid nanofluids.

$$Viscosity = 144.56\text{-}2.6242*A - 9.38*B\text{-}0.158*C + 0.188*A*B - 2.168E\text{-}003*A*C + 0.238*B*C + 0.018*A^2 + 10.138*B^2 + 0.038*C^2 \quad (4)$$

In Fig. 4(a), we observe a normal plot of residuals for the viscosity data of CuO-polyaniline/palm oil hybrid nanofluids. This graph illustrates that all the data points align along a single straight line, indicating that the residual values possess an appropriate standard error term. In a well-fitted model, data points should not exhibit any discernible pattern; instead, they should closely approximate a straight line. The normal plot of residuals clearly demonstrates that the data points do not adhere to any specific trend and instead cluster near the straight line, confirming that the distribution is random.

To further mitigate any deviations in the data points, an outlier plot is presented in Fig. 4(b). This plot is used to identify any data points that fall outside the acceptable range (±3.0 standard deviations), suggesting their unreliability. Fig. 4(b) illustrates that all data points remain within the permissible range, affirming the data's reliability.

The comparison between the estimated viscosity obtained from the developed mathematical model and the actual experimental data is illustrated in Fig. 5. Notably, a 45-degree diagonal line running through the center of the graph aligns perfectly with all the plotted data points. This alignment signifies an outstanding agreement between the predicted values and the actual data. It serves as strong confirmation of the reliability and accuracy of the regression equation generated for predicting the response variable.

Fig. 6 provides a comprehensive visual analysis of the relationships between key variables, namely temperature, volume concentration and CuO composition to viscosity of nanofluids, as represented through both contour and 3D surface plots. The contour plots (Fig. 6(a-c)) shed light on the influence of these variables on nanofluid viscosity. Notably, higher concentrations of nanoadditives in the palm oil are associated with elevated viscosity while lower temperatures also contribute to increased viscosity. Meanwhile, CuO composition has a relatively minor impact on the changes in the viscosity of nanofluids when compared to the factors of volume concentration and temperature.

Delving deeper into the 3D surface plots (Fig. 6(d-f)) reinforces these observations. It becomes evident that variations in CuO composition have limited effects on nanofluid viscosity when contrasted with changes in volume concentration and testing temperature. Specifically, adjustments in volume concentration wield a more pronounced influence on viscosity, with Fig. 6(d) revealing that higher viscosity is achieved by increasing volume concentration, particularly at lower temperatures. This phenomenon can be attributed to the heightened intensity of Brownian motion within the nanofluid system, as previously noted [41,42]. The lower viscosity observed at elevated temperatures is likely a result of hydrodynamic interactions among solid additives [43,44]. This interaction arises from the disturbance created by one particle within the base fluid affecting neighboring particles, especially at higher volume concentrations. Notably, an increase in the volume concentration of nanoparticles was observed to elevate the viscosity of the nanofluids [45–47]. This effect can be attributed to the formation of more symmetrical and larger clusters of nanoparticles, driven by van der Waals forces between the nanoparticles and the base fluid. Furthermore, a higher dispersion of nanoparticles led to more pronounced shear stress between fluid layers, resulting in an overall increase in viscosity [48–50]. In summary, the contour and 3D surface plots collectively underscore the significance of controlling nanoparticle concentration and testing temperature as paramount factors impacting nanofluid viscosity. Conversely, CuO composition appears to play a comparatively minor role in influencing viscosity, as corroborated by the contour plot and 3D surface plot analysis.

3.3. Influence of independent variables on thermal conductivity of copper oxide-polyaniline/palm oil hybrid nanofluids

In Table 5, we find a succinct summary of the valuable contributions made by each individual term within the developed mathematical model, as represented in Equation (5). The table draws attention to the impressive F-value of 1244.2, coupled with a corresponding P-value of less than 0.05. These findings unequivocally establish the significance of the proposed model. According to the main model, terms A, B and C were shown to have a considerable impact on thermal conductivity of nanofluids. Furthermore, through the ANOVA, we gain confidence in the reliability of the proposed equation by examining R^2 (the coefficient of determination) and

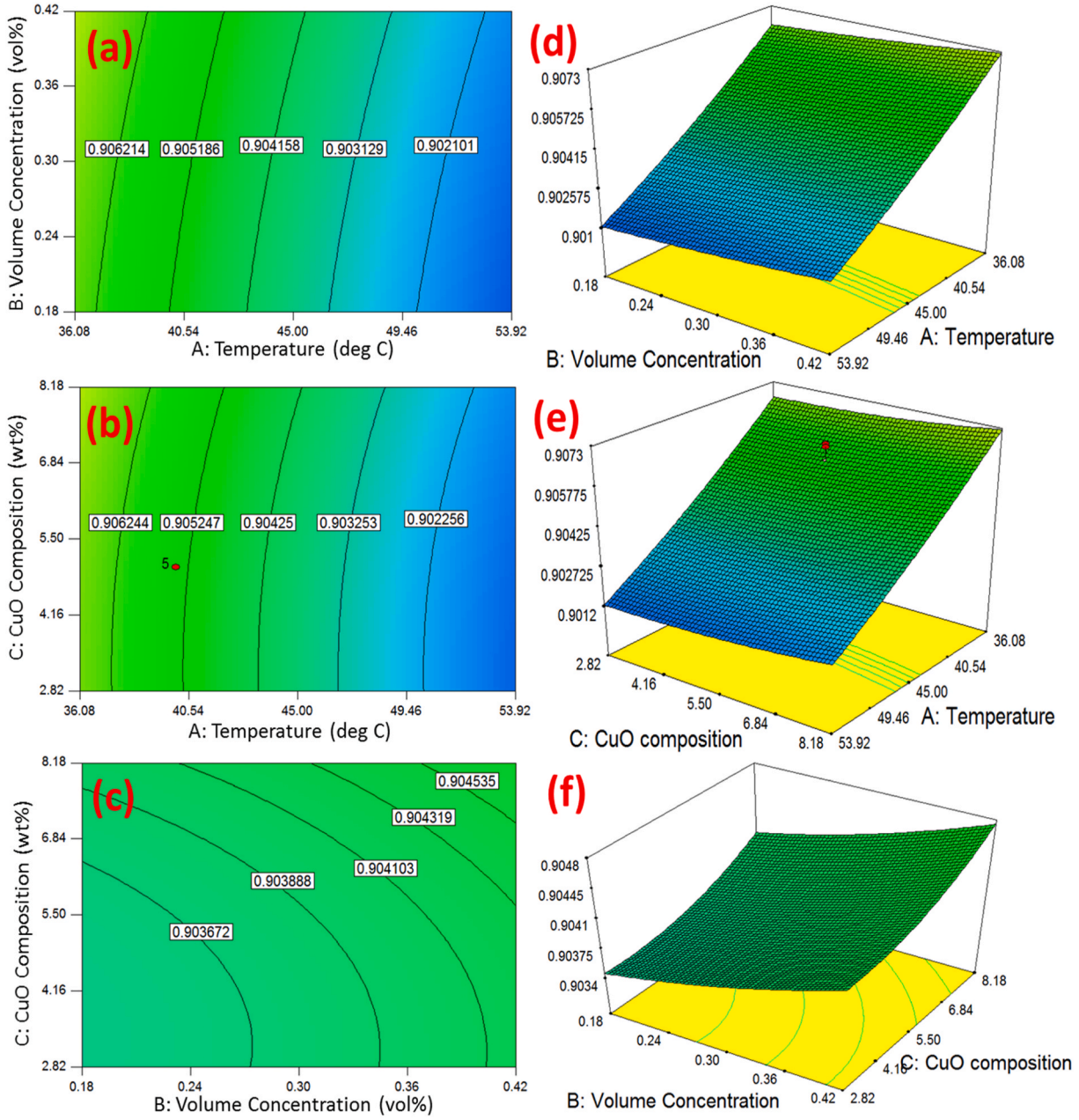

Fig. 3. Contour plot and 3D surface plot of density for CuO-polyaniline/palm oil hybrid nanofluids as a function of (a), (d) temperature and volume concentration, (b), (e) temperature and CuO composition, (c), (f) volume concentration and CuO composition.

standard deviation. Remarkably, R^2 stands at 0.9991, signifying that the proposed regression equation can account for a remarkable 99.91 % of the total variation observed in the data. Moreover, the standard deviation, at 1.95E-03, further bolsters the equation's reliability. To underscore this, predicted R^2 and adjusted R^2 values, amounting to 99.32 % and 99.83 %, respectively, affirm a high degree of dependable agreement in the model's predictions.

$$\textit{Thermal conductivity} = 0.14 + 1.81E\text{-}003*A - 0.02*B - 7.64E\text{-}004*C + 2.64E\text{-}003*A*B + 1.46E\text{-}005*A*C + 9.83E\text{-}004*B*C + 2.56E\text{-}005*A^2 - 0.05*B^2 - 7.8E\text{-}005*C^2 \quad (5)$$

In Fig. 7(a), we can observe a normal plot of residuals depicting the thermal conductivity data for CuO-polyaniline/palm oil hybrid nanofluids. This graph effectively demonstrates that all data points align neatly along a single straight line, indicating that the residual values adhere to an appropriate standard error term. In a well-fitted model, data points should not display any noticeable pattern; instead, they should closely approximate a straight line. The normal plot of residuals unequivocally establishes that the data points do

Table 4
The viscosity's empirical model results using ANOVA.

Parameter	Sum of square	Degree of freedom	Mean Squares	F value	P-value	
Model	4333.48	9	481.5	1550.05	<0.0001	significant
A-Temperature	3723.48	1	3723.48	11986.7	<0.0001	
B-Volume Concentration	11.91	1	11.91	38.35	0.0001	
C–CuO composition	5.91	1	5.91	19.01	0.0014	
AB	1.08	1	1.08	3.47	0.092	
AC	0.076	1	0.076	0.24	0.632	
BC	0.36	1	0.36	1.15	0.308	
A^2	21.46	1	21.46	69.09	<0.0001	
B^2	0.52	1	0.52	1.68	0.2243	
C^2	1.48	1	1.48	4.78	0.0537	
Residual	3.11	10	0.31			
Lack of Fit	3.06	5	0.61	62.88	0.0002	significant
Pure Error	0.049	5	9.73E-03			
Correlation Total	4336.58	19				
Standard Deviation	0.56	R-Squared	0.9993			
Mean	56.89	Adj R-Squared	0.9986			
C.V. %	0.98	Pred R-Squared	0.9923			
PRESS	33.58	Adeq Precision	127.448			

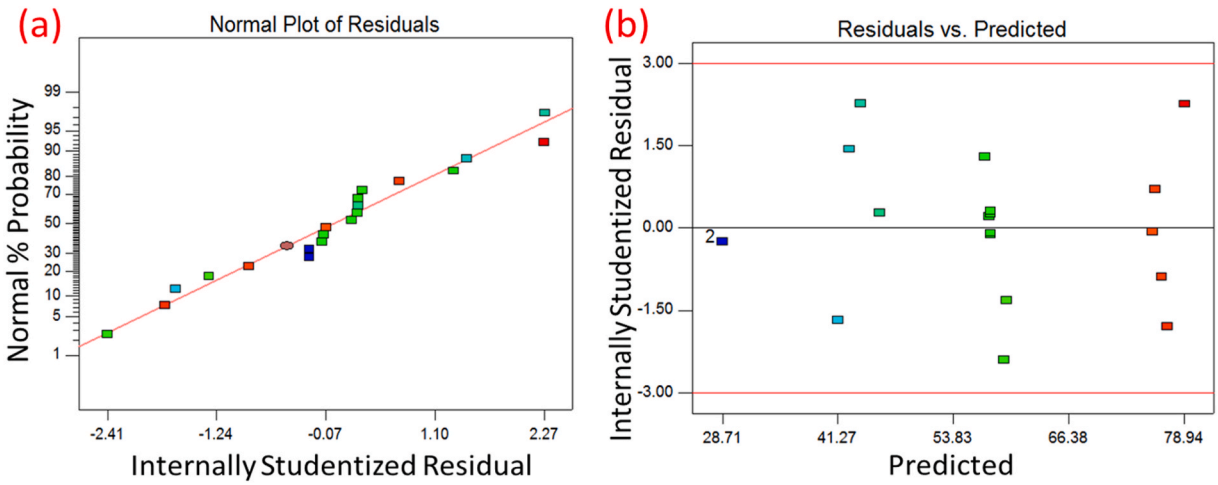

Fig. 4. Model's adequacy tests for viscosity; (a) Normal residual plot, (b) Outlier plot.

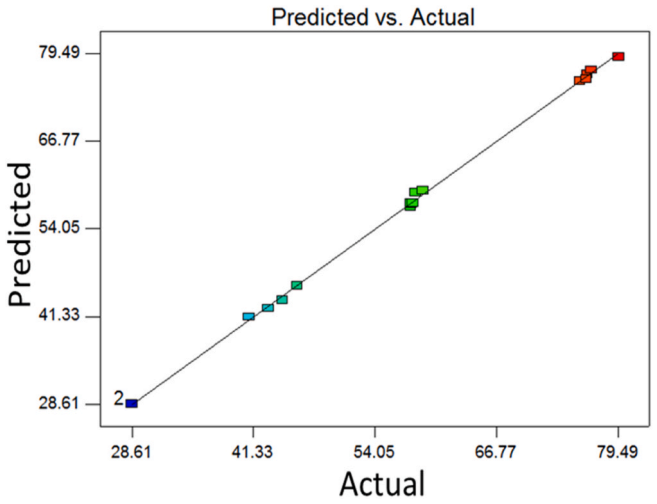

Fig. 5. Predicted vs. actual plot on viscosity of CuO-polyaniline/palm oil hybrid nanofluids.

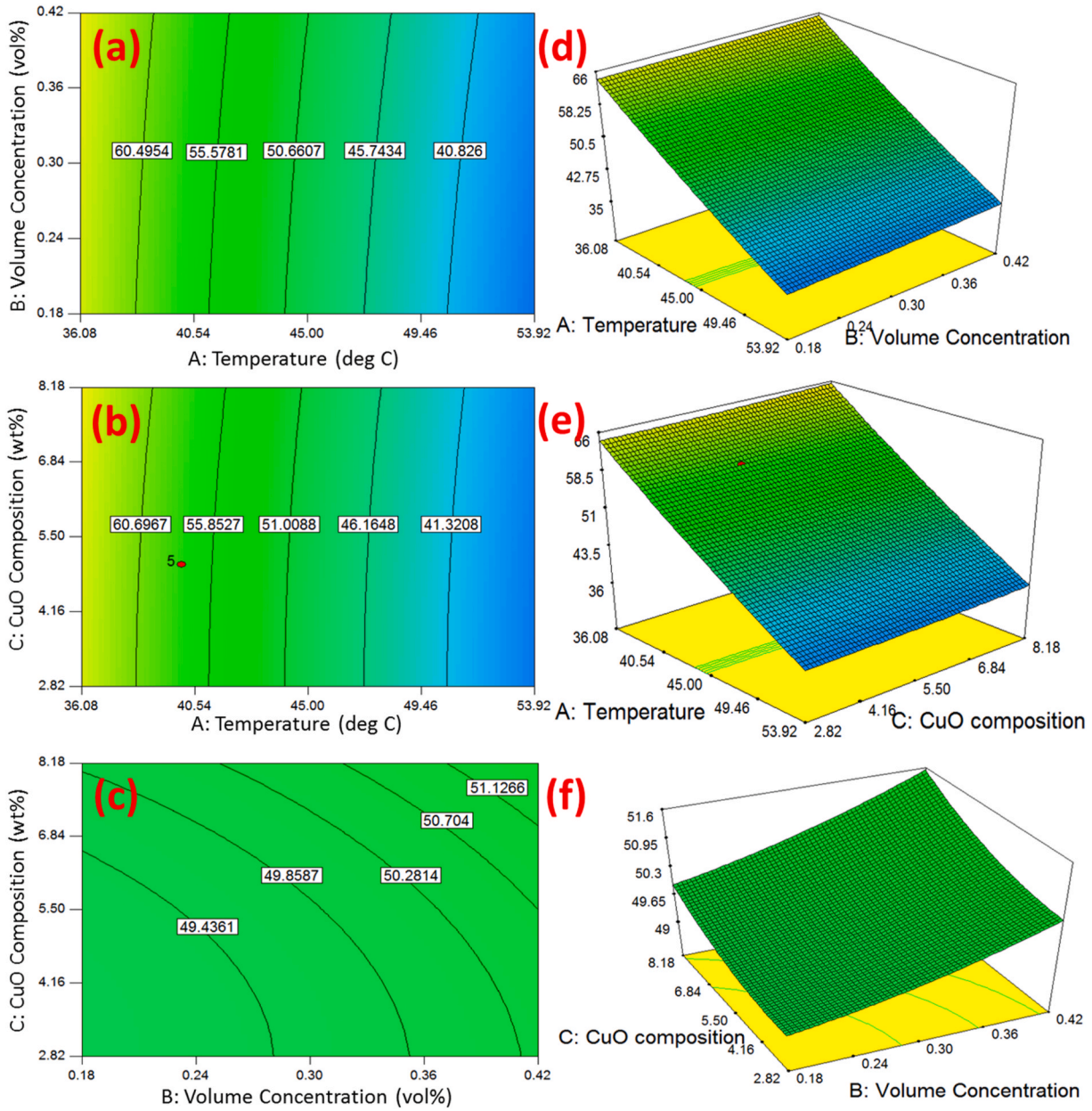

Fig. 6. Contour plot and 3D surface plot of viscosity for CuO-polyaniline/palm oil hybrid nanofluids as a function of (a), (d) temperature and volume concentration, (b), (e) temperature and CuO composition, (c), (f) volume concentration and CuO composition.

not follow any discernible trend and, instead, cluster closely around the straight line. This robustly confirms that the distribution of residuals is indeed random.

To provide further assurance against potential deviations in the data, Fig. 7(b) showcases an outlier plot. The purpose of this plot is to identify any data points that fall outside the accepted range, typically defined as ±3.0 standard deviations, which may indicate their unreliability or outlier status. Fig. 7(b) effectively demonstrates that all data points remain comfortably within this permissible range, thereby affirming the overall reliability and credibility of the dataset.

Fig. 8 presents a direct comparison between the estimated thermal conductivity values obtained from our developed mathematical model and the corresponding actual experimental data. A noteworthy feature of this graph is the presence of a precisely aligned 45-degree diagonal line that passes through the center, impeccably intersecting with all the data points plotted. This remarkable alignment serves as compelling evidence of an exceptional agreement between the predicted thermal conductivity values and the observed experimental data. It provides robust affirmation of the reliability and accuracy of the regression equation that was formulated to predict the response variable, underlining the model's strong predictive capability.

Table 5
The thermal conductivity's empirical model results using ANOVA.

Parameter	Sum of square	Degree of freedom	Mean Squares	F value	P-value	
Model	0.043	9	4.73E-03	1244.2	<0.0001	significant
A-Temperature	0.037	1	0.037	9861.48	<0.0001	
B-Volume Concentration	1.67E-03	1	1.67E-03	439.36	<0.0001	
C–CuO composition	6.91E-05	1	6.91E-05	18.2	0.0016	
AB	2.24E-04	1	2.24E-04	58.88	<0.0001	
AC	3.47E-06	1	3.47E-06	0.91	0.3619	
BC	6.28E-06	1	6.28E-06	1.65	0.2274	
A^2	1.11E-04	1	1.11E-04	29.29	0.0003	
B^2	1.31E-05	1	1.31E-05	3.44	0.0931	
C^2	7.69E-06	1	7.69E-06	2.02	0.1853	
Residual	3.80E-05	10	3.80E-06			
Lack of Fit	2.82E-05	5	5.63E-06	2.87	0.1359	not significant
Pure Error	9.81E-06	5	1.96E-06			
Correlation Total	0.043	19				
Standard Deviation	1.95E-03	R-Squared	0.9991			
Mean	0.29	Adj R-Squared	0.9983			
C.V. %	0.68	Pred R-Squared	0.9932			
PRESS	2.90E-04	Adeq Precision	119.741			

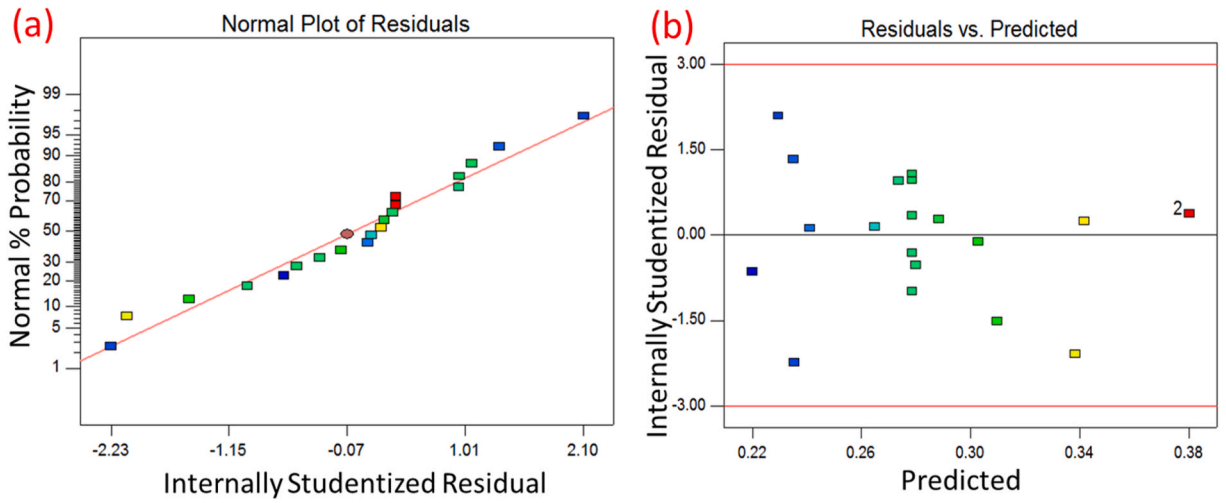

Fig. 7. Model's adequacy tests for thermal conductivity; (a) Normal residual plot, (b) Outlier plot.

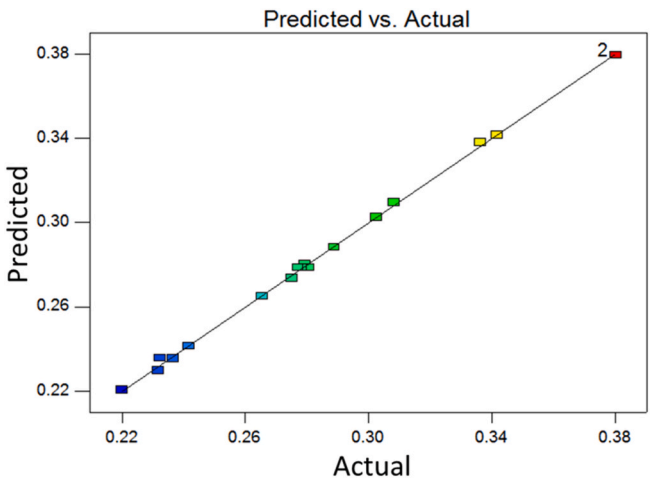

Fig. 8. Predicted vs. actual plot on thermal conductivity of CuO-polyaniline/palm oil hybrid nanofluids.

Fig. 9 offers a comprehensive visual examination of the interrelationships among key variables: temperature, volume concentration, CuO composition, and thermal conductivity. These relationships are explored through both contour and 3D surface plots. The contour plots (Fig. 9(a-c)) unveil the impact of these variables on nanofluid thermal conductivity. Notably, higher concentrations of nanoadditives within palm oil correspond to increased thermal conductivity. Additionally, higher temperatures contribute to higher thermal conductivity. However, the influence of CuO composition on nanofluid thermal conductivity is comparatively modest when contrasted with the potency of volume concentration and temperature factors. The slightly increment in thermal conductivity effected by CuO composition can be attributed to a higher percentage of CuO nanoparticles being finely embedded within the polyaniline matrix through the polymerization process.

Delving into the 3D surface plots (Fig. 9(d-f)) reinforces these findings. It becomes evident that variations in CuO composition have

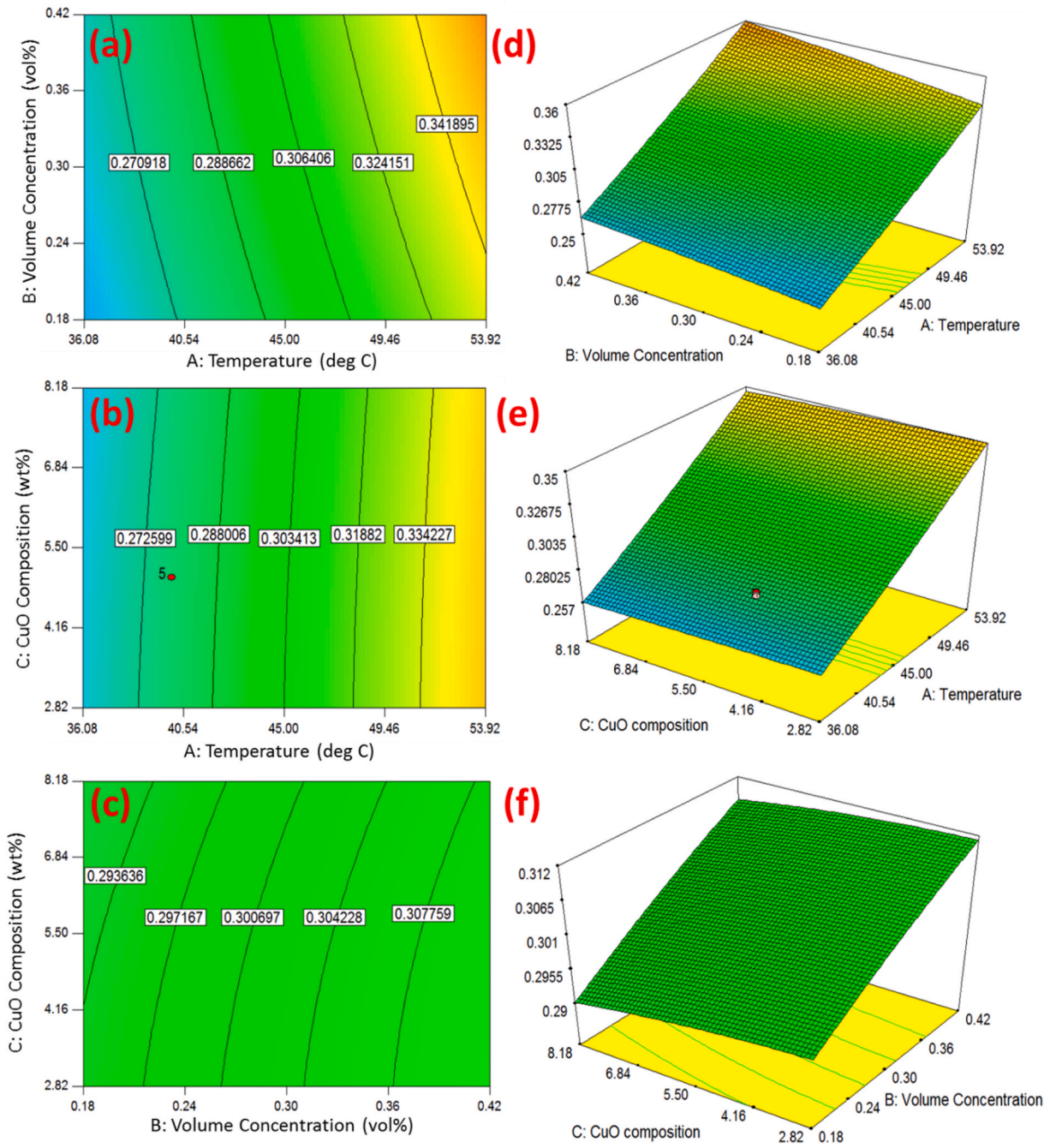

Fig. 9. Contour plot and 3D surface plot of thermal conductivity for CuO-polyaniline/palm oil hybrid nanofluids as a function of (a), (d) temperature and volume concentration, (b), (e) temperature and CuO composition, (c), (f) volume concentration and CuO composition.

slightly enhance the thermal conductivity of nanofluid. Specifically, adjustments in volume concentration exert a more pronounced influence on thermal conductivity, with Fig. 9(d) demonstrating that higher thermal conductivity is attained through increased volume concentration and temperatures.

The higher thermal conductivity observed at higher volume concentration can be attributed to the interaction and binding of nanoparticles become more pronounced in the presence of a high volume concentration of CuO-polyaniline nanocomposites. This phenomenon intensifies heat energy transfer through Brownian motion [51–53]. Additionally, the molecular layer of the base liquid surrounding the dispersed nanoparticles plays a role in improving heat transfer properties through the solid-liquid interphase [54,55]. Furthermore, the thermal conductivity of the solid additives themselves also contributes to the enhancement of nanofluids' thermal conductivity [56,57].

In summary, the contour and 3D surface plots collectively underscore the significance of controlling nanoparticle concentration and testing temperature as primary factors affecting nanofluid thermal conductivity. Conversely, CuO composition appears to have a comparatively minor role in influencing thermal conductivity, as validated by the contour plot and 3D surface plot analyses.

3.4. Multi-objective optimization of density, viscosity and thermal conductivity of copper oxide-polyaniline/palm oil hybrid nanofluids

Multi-objective optimization using Response Surface Methodology (RSM) serves as a graphical tool to validate optimal values for multiple manipulated variables, either minimizing or maximizing response variables. It effectively illustrates the relationship between manipulated variables and response variables, providing essential insights into the sensitivity of specific responses concerning changes in independent variables. The primary advantage of employing RSM lies in its capacity to fine-tune input constraints to optimize specific responses [26,43].

The preceding sections have highlighted that increasing temperature and volume concentration enhances the thermal conductivity properties of CuO-polyaniline-palm oil nanofluids. However, density and viscosity exhibit contrasting trends with thermal conductivity. Both density and viscosity show a decreasing trend with respect to temperature but increase with the volume concentration of CuO-polyaniline nanoadditives. This research aims to identify the best combination of density, viscosity, and thermal conductivity for the studied nanofluids.

Table 6 presents the data related to the optimization of density, viscosity, and thermal conductivity, including the objective function, the parameter ranges affecting factors, and the optimization cases. To maximize thermal conductivity while minimizing density and viscosity in CuO-polyaniline/palm oil nanofluids, the temperature range was selected from 36.08 to 53.92, the volume concentration range from 0.18 to 0.42, and the CuO composition range from 2.82 to 8.18. The optimization plot illustrating the thermal physical behavior of nanofluids is presented in Fig. 10. The optimum values obtained from the best solution are 0.901532 g/mL for density, 37.1229 mPa s for viscosity, and 0.356891 W/mK for thermal conductivity, with temperature of 53.92 °C, volume concentration of 0.38 vol% and CuO composition of 2.90 wt%.

3.5. Economic analysis via price performance factor (PPF) evaluation

Research publications have shed light on a significant challenge in the practical application of nanotechnology, particularly in engineering and industrial contexts, which is the high cost associated with nanoadditives. Several factors contribute to this elevated cost, including the expensive synthesis of raw materials for nanoadditives, the necessity for nanoadditives to have an exceptionally high purity of 99.99 %, the use of advanced technology instruments and costly procedures for the synthesis of nanoadditives, and the limited production of nanoadditives due to specialized approaches required in their manufacturing process [58,59]. When the production expenses for nanoadditives are high, the formulation of nanofluids for heat transfer applications also becomes prohibitively expensive. For a comprehensive assessment of budgets and the benefits of nanofluid systems, it is essential to consider the cost of formulating nanofluids. In fact, US Research Nanomaterials, in 2017, provided insights into the cost of formulated nanofluids to facilitate a more accurate evaluation of the overall expenses and advantages associated with nanofluid systems [60].

Fig. 11 offers insights into the relationship between the relative thermal conductivity of CuO-polyaniline/palm oil hybrid nanofluids and the associated preparation costs at varying volume concentrations of nanoadditives and temperatures. Notably, it's observed that the cost of nanofluids tends to rise with increasing volume concentration of nanoadditives, a trend depicted in Fig. 11 across all investigated temperatures. Fig. 11(a) specifically shows the relative thermal conductivity of CuO-polyaniline/palm oil nanofluids at different volume concentrations at 30 °C. Here, we see that the relative thermal conductivity increases with a higher dispersion of CuO-polyaniline nanocomposites, primarily due to the heightened impact of Brownian motion within the nanofluid system. In Fig. 11(b–d), the relative thermal conductivity is observed to increase with the volume concentration of nanoadditives; however, it experiences a significant decline at higher temperatures. Specifically, the relative thermal conductivity is found to be in the range of 1.3–1.55 at elevated temperatures (40, 50, and 60 °C), whereas it remains in the range of 1.85–2.1 at 30 °C. The decrease in relative thermal conductivity between temperatures 40–60 °C is attributed to the lower enhancement of thermal conductivity as compared to palm oil as the temperature rises.

Theoretically, more cost-effective nanofluids should combine lower production expenses with significant improvements in heat transfer behavior. However, the results suggest that the studied nanofluids may not be economically advantageous, as the enhancement in thermal conductivity is relatively modest in comparison to the nanofluids' price.

To delve further into the economic evaluation of the CuO-polyaniline/palm oil nanofluids at the studied parameters, the calculation of the Price Performance Factor (PPF) is presented in Fig. 12(a–d). The PPF values demonstrate a decrease with increasing volume concentration of nanoadditives. This consistent trend is observed across all the PPF vs volume concentration graphs at different temperatures, indicating that the CuO-polyaniline/palm oil nanofluids under the studied conditions may not necessarily be economically favorable.

Table 6
Input factors of objective function.

Name of input	Desire goal	Limits		Weight	
		Lower	Upper	Lower	Upper
Temperature	is in range	36.0809	53.9191	1	1
Volume Concentration	is in range	0.181079	0.418921	1	1
CuO composition	is in range	2.82428	8.17572	1	1
Density	minimize	0.8999	0.91069	1	1
Viscosity	minimize	28.613	79.492	1	1
Thermal conductivity	maximize	0.2174	0.3835	1	1

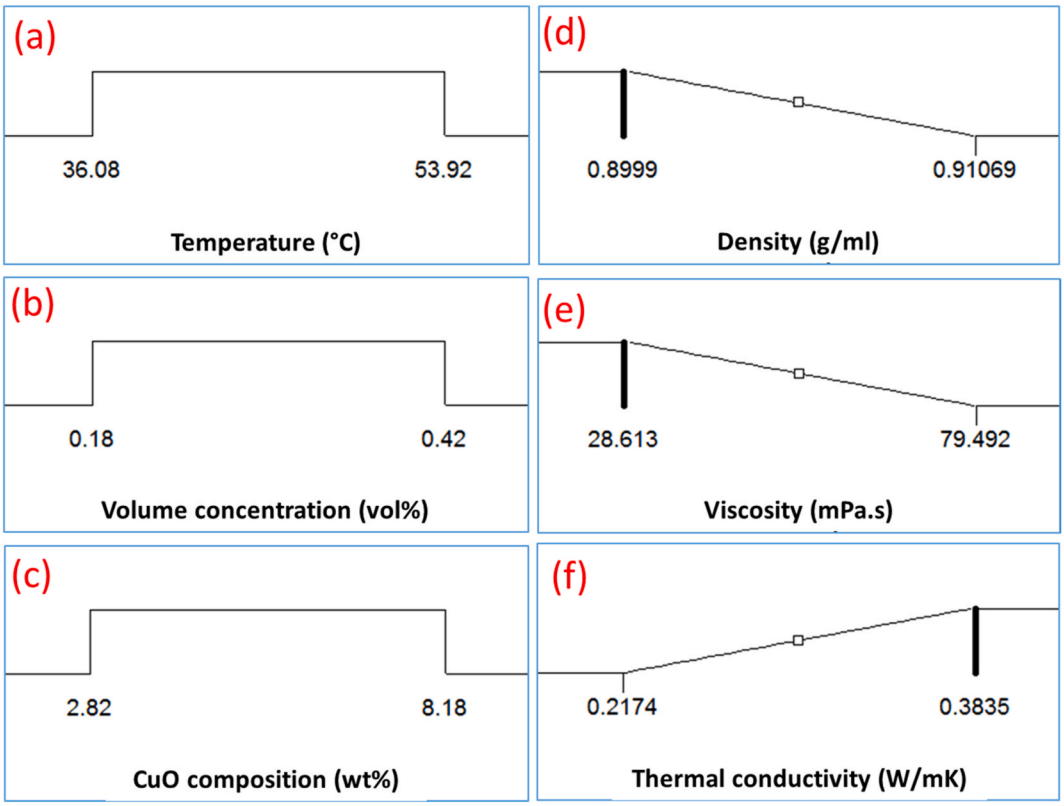

Fig. 10. Optimization plot of the thermal physical properties of CuO-polyaniline/palm oil hybrid nanofluids.

To enhance the PPF and make these nanofluids more viable for potential coolants in fuel cell devices, there is a need for greater improvements in thermal conductivity properties. This analysis underscores the importance of economic assessments in understanding the viability of formulated nanofluids. Such assessments can provide valuable guidelines for future research, allowing for adjustments and modifications to various parameters in nanofluid formulation, such as nanoadditive morphology, dimensions, and surfactant dispersion, to enhance stability and overall nanofluid performance [61–63].

4. Conclusions

This research focuses on formulating CuO-polyaniline/palm oil hybrid nanofluids as a potential coolants for fuel cell technology, and investigating their density, viscosity, and thermal conductivity properties within the ranges of 0.1–0.5 vol% volume concentration, 30–60 °C temperature and 1–10 wt% of CuO composition. The author have developed a mathematical model to predict and validate the optimal thermophysical properties of the nanofluid. Here are the key findings and discussions.

- The study reveals that variations in CuO composition exhibit minimal influence on the density of CuO-polyaniline/palm oil hybrid nanofluids, whereas higher nanoadditive concentrations and lower testing temperatures significantly elevate nanofluid density, highlighting the substantial impact of volume concentration and temperature compared to CuO composition on the overall nanofluid density changes.

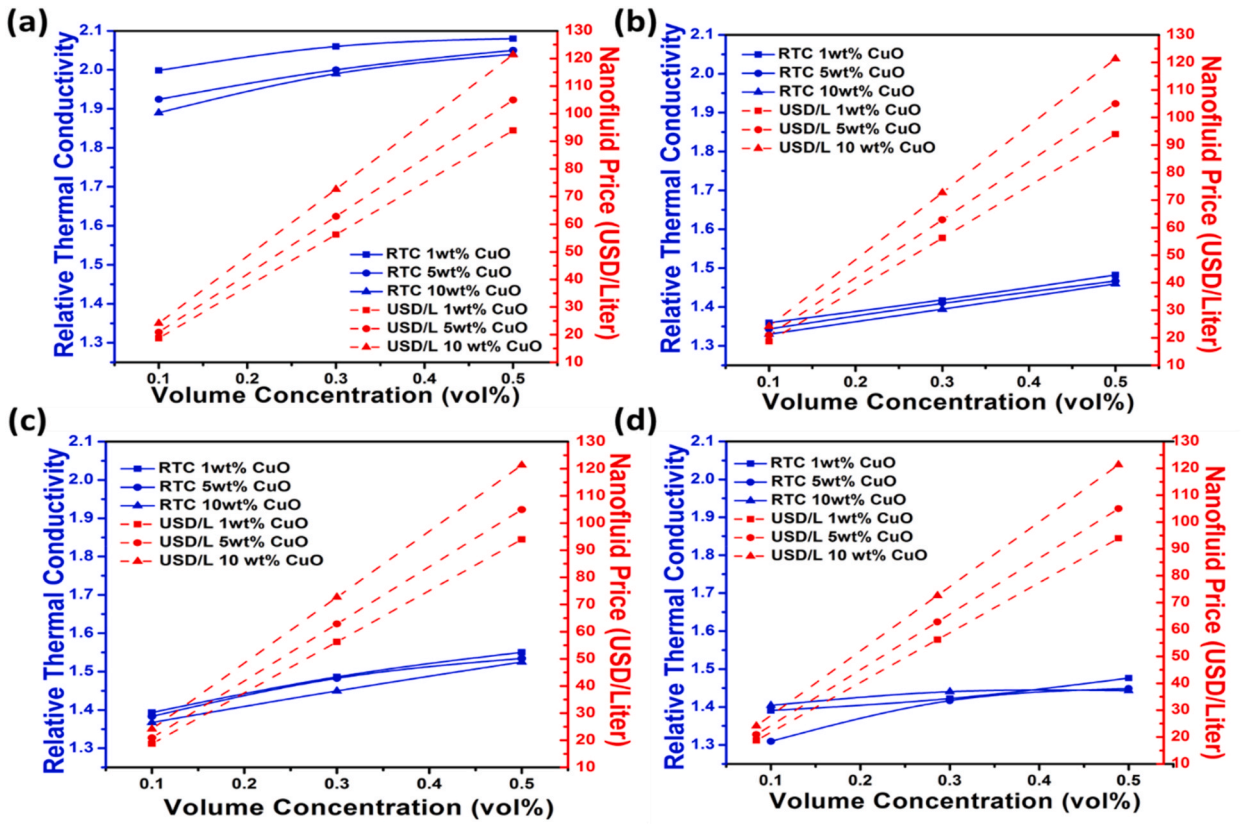

Fig. 11. Relative thermal conductivity and price of CuO-polyaniline/palm oil hybrid nanofluids at different temperature (a) 30 °C, (b) 40 °C, (c) 50 °C and (d) 60 °C.

- Nanofluids exhibited maximum viscosity with 0.5 vol% of dispersed nanoadditives in palm oil, but their viscosity decreased at higher temperatures. CuO composition has a relatively minor impact on the changes in the viscosity CuO-polyaniline/palm oil hybrid nanofluids
- The highest volume concentration, 0.5 vol% exhibits the highest thermal conductivity compared to others. The most enhanced heat transfer behavior was achieved by nanofluid containing 10 wt% CuO-polyaniline nanocomposites.
- The RSM approach proved successful in predicting the density, viscosity, and thermal properties of nanofluids based on the temperature, volume percentage of nanoadditives and CuO composition.
- The exceptional agreement between the predicted and actual data, as evidenced by the formation of a 45° angle line in the predicted vs. actual data graph and the commendable R^2 values of 98.66 % for density, 99.93 % for viscosity, and 99.91 % for thermal conductivity models, serves to validate the reliability of the generated regression equations for predicting responses.
- The optimal density, viscosity, and thermal conductivity of polyaniline-palm oil nanofluids were found to be 0.901532 g/mL, 37.1229 mPa s, and 0.356891 W/mK, respectively. The critical parameters for achieving these values were a temperature of 53.92 °C, a volume concentration of 0.38 vol% for nanoadditives and 2.90 wt% of CuO composition.
- The evaluation of the Price Performance Factor (PPF) indicated that the studied CuO-polyaniline/palm oil hybrid nanofluids at these parameters are not cost-effective, as the PPF graph showed a decrease in PPF value with increasing volume concentration.

CRediT authorship contribution statement

A.G.N. Sofiah: Conceptualization, Data curation, Formal analysis, Investigation, Methodology, Writing – original draft, Writing – review & editing. **J. Pasupuleti:** Funding acquisition, Project administration, Supervision, Writing – review & editing. **M. Samykano:** Resources, Supervision, Writing – review & editing. **R. Kumar Rajamony:** Validation, Visualization. **A.K. Pandey:** Resources, Supervision. **Nur Fatin Sulaiman:** Formal analysis, Methodology, Software. **Zatil Amali Che Ramli:** Formal analysis, Validation. **S.K. Tiong:** Funding acquisition. **S.P. Koh:** Funding acquisition.

Declaration of competing interest

The authors declare that they have no known competing financial interests or personal relationships that could have appeared to influence the work reported in this paper.

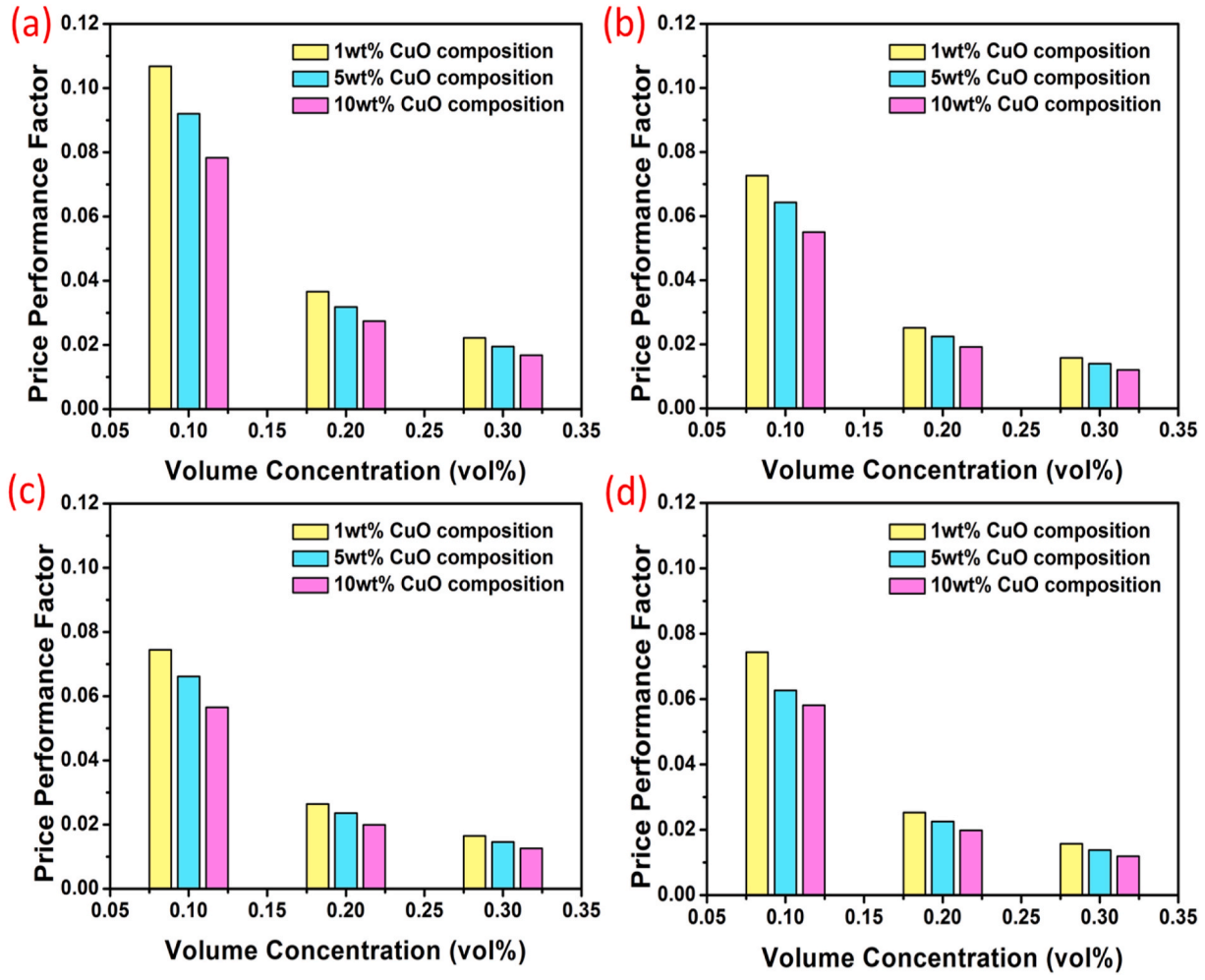

Fig. 12. Price performance factor for CuO-polyaniline/palm oil hybrid nanofluids at different temperature (a) 30 °C, (b) 40 °C, (c) 50 °C and (d) 60 °C.

Data availability

No data was used for the research described in the article.

Acknowledgement

This work was supported by the Ministry of Higher Education of Malaysia through the HICoE grant (2022001HICOE), Dato' Low Tuck Kwong International Energy Transition Grant (202203004ETG), AAIBE Chair of Renewable Energy (202202KETTHA) as well as Tenaga Nasional Berhad (TNB) and UNITEN through the BOLD Refresh Publication Fund under the project code of J510050002-IC-6 BOLDREFRESH2025-Center of Excellence.

Appendix A. Supplementary data

Supplementary data to this article can be found online at https://doi.org/10.1016/j.csite.2023.103931.

References

[1] F. Alanazi, Electric vehicles: benefits, challenges, and potential solutions for widespread adaptation, Appl. Sci. 13 (10) (2023) 6016.
[2] A. Karki, et al., Status of pure electric vehicle power train technology and future prospects, Applied System Innovation 3 (3) (2020) 35.
[3] M. Singh, D. Zappa, E. Comini, Solid oxide fuel cell: decade of progress, future perspectives and challenges, Int. J. Hydrogen Energy 46 (54) (2021) 27643–27674.
[4] E. Cabrera, J.M.M. de Sousa, Use of sustainable fuels in aviation—a Review, Energies 15 (7) (2022) 2440.
[5] S. Chakraborty, et al., Hydrogen energy as future of sustainable mobility, Front. Energy Res. 10 (2022), 893475.

[6] N. Sazali, et al., New perspectives on fuel cell technology: a brief review, Membranes 10 (5) (2020) 99.
[7] T.B. Ferriday, P.H. Middleton, Alkaline fuel cell technology-A review, Int. J. Hydrogen Energy 46 (35) (2021) 18489–18510.
[8] S. Asghari, H. Akhgar, B.F. Imani, Design of thermal management subsystem for a 5 kW polymer electrolyte membrane fuel cell system, J. Power Sources 196 (6) (2011) 3141–3148.
[9] M.H. Bargal, et al., Liquid cooling techniques in proton exchange membrane fuel cell stacks: a detailed survey, Alex. Eng. J. 59 (2) (2020) 635–655.
[10] M. Ramezanizadeh, et al., A review on the approaches applied for cooling fuel cells, Int. J. Heat Mass Tran. 139 (2019) 517–525.
[11] I. Dhuchakallaya, P. Saechan, Enhancing the cooling efficiency of the air cooling system for electric vehicle battery modules through liquid spray integration, J. Energy Storage 72 (2023), 108751.
[12] M. Hemmat Esfe, M. Afrand, A review on fuel cell types and the application of nanofluid in their cooling, J. Therm. Anal. Calorim. 140 (2020) 1633–1654.
[13] E.T. Sayed, et al., Augmenting performance of fuel cells using nanofluids, Therm. Sci. Eng. Prog. 25 (2021), 101012.
[14] I. Zakaria, et al., Heat transfer and electrical discharge of hybrid nanofluid coolants in a fuel cell cooling channel application, Appl. Therm. Eng. 210 (2022), 118369.
[15] T. Yusaf, et al., Sustainable hydrogen energy in aviation – a narrative review, Int. J. Hydrogen Energy 52 (2023) 1026–1045.
[16] M.C. Williams, J.P. Strakey, W.A. Surdoval, The US department of energy, office of fossil energy stationary fuel cell program, J. Power Sources 143 (1–2) (2005) 191–196.
[17] S. Talib, et al., Thermophysical properties of silicon dioxide (SiO2) in ethylene glycol/water mixture for proton exchange membrane fuel cell cooling application, Energy Proc. 79 (2015) 366–371.
[18] R. Islam, B. Shabani, Prediction of electrical conductivity of TiO2 water and ethylene glycol-based nanofluids for cooling application in low temperature PEM fuel cells, Energy Proc. 160 (2019) 550–557.
[19] J. Siriworachanyadee, et al., The polarization and depolarization current characteristics of mineral oil, natural ester (FR3), palm oil, and liquid impregnated pressboard, in: IEEE 20th International Conference on Dielectric Liquids (ICDL), IEEE, 2019.
[20] M.H. Esfe, et al., Experimental study and viscosity modeling by adding oxide nanoparticles to oil to improve the performance, Tribol. Int. 190 (2023), 109031.
[21] M.H. Esfe, et al., Presenting the best correlation relationship for predicting the dynamic viscosity of CuO nanoparticles in ethylene glycol-Water base fluid using response surface methodology, Arab. J. Chem. (2023), 105467.
[22] F. Sahin, M.C. Acar, O. Genc, Experimental determination of NiFe2O4-water nanofluid thermophysical properties and evaluation of its potential as a coolant in polymer electrolyte membrane fuel cells, Int. J. Hydrogen Energy 50 (2023) 1572–1583.
[23] Y.T. Kang, H.J. Kim, K.I. Lee, Heat and mass transfer enhancement of binary nanofluids for H2O/LiBr falling film absorption process, Int. J. Refrig. 31 (5) (2008) 850–856.
[24] F. Pourfayaz, et al., Process development and exergy analysis of a novel hybrid fuel cell-absorption refrigeration system utilizing nanofluid as the absorbent liquid, Int. J. Refrig. 97 (2019) 31–41.
[25] M. Kordi, A.J. Moghadam, E. Afshari, Effects of cooling passages and nanofluid coolant on thermal performance of polymer electrolyte membrane fuel cells, Journal of Electrochemical Energy Conversion and Storage 16 (3) (2019), 031001.
[26] M. Khani, et al., Novel α-alumina@ CuO-Fe2O3nanofluid for potential application in PEM fuel cell cooling systems: towards neutralizing the increase of electrical conductivity, Thermochim. Acta 695 (2021), 178818.
[27] G. Tourillon, et al., Dispersive X-ray spectroscopy for time-resolved in situ observation of electrochemical inclusion of metallic clusters within a conducting polymer, Phys. Rev. Lett. 57 (5) (1986) 603.
[28] S. Shahabuddin, et al., SrTiO3 nanocube-doped polyaniline nanocomposites with enhanced photocatalytic degradation of methylene blue under visible light, Polymers 8 (2) (2016) 27.
[29] A. Sofiah, et al., A comparative experimental study on the physical behavior of mono and hybrid RBD palm olein based nanofluids using CuO nanoparticles and PANI nanofibers, Int. Commun. Heat Mass Tran. 120 (2021), 105006.
[30] A.G.N. Sofiah, et al., Multi-objective optimization and price performance factor evaluation of polyaniline nanofibers-palm oil nanofluids for thermal energy storage application, Case Stud. Therm. Eng. 52 (2023), 103673.
[31] J. Li, et al., Multi-objective optimization of mini U-channel cold plate with SiO2 nanofluid by RSM and NSGA-II, Energy 242 (2022), 123039.
[32] M.H. Esfe, S. Alidoust, D. Toghraie, Comparison of the thermal conductivity of hybrid nanofluids with a specific proportion ratio of MWCNT and TiO2 nanoparticles based on the price performance factor, Mater. Today Commun. 34 (2023), 105411.
[33] A. Alirezaie, et al., Price-performance evaluation of thermal conductivity enhancement of nanofluids with different particle sizes, Appl. Therm. Eng. 128 (2018) 373–380.
[34] M.H. Esfe, et al., Thermal conductivity of MWCNT-TiO2/Water-EG hybrid nanofluids: calculating the price performance factor (PPF) using statistical and experimental methods (RSM), Case Stud. Therm. Eng. 48 (2023), 103094.
[35] A.B. Mahfouz, et al., Optimization of viscosity of titania nanotubes ethylene glycol/water-based nanofluids using response surface methodology, Fuel 347 (2023), 128334.
[36] M. Hojjat, Nanofluids as coolant in a shell and tube heat exchanger: ANN modeling and multi-objective optimization, Appl. Math. Comput. 365 (2020), 124710.
[37] Z. Said, et al., Synthesis, stability, density, viscosity of ethylene glycol-based ternary hybrid nanofluids: experimental investigations and model-prediction using modern machine learning techniques, Powder Technol. 400 (2022), 117190.
[38] A. Sofiah, et al., Copper oxide/polyaniline nanocomposites-blended in palm oil hybrid nanofluid: thermophysical behavior evaluation, J. Mol. Liq. 375 (2023), 121303.
[39] M. Jamei, et al., Estimating the density of hybrid nanofluids for thermal energy application: application of non-parametric and evolutionary polynomial regression data-intelligent techniques, Measurement 189 (2022), 110524.
[40] M.H. Esfe, et al., Optimization of density and coefficient of thermal expansion of MWCNT in thermal oil nanofluid and modeling using MLP and response surface methodology, Tribol. Int. 183 (2023), 108410.
[41] A. Sofiah, et al., Copper (II) oxide nanoparticles as additives in RBD palm olein: experimental analysis and mathematical modelling, J. Mol. Liq. 363 (2022), 119892.
[42] A. Sofiah, et al., An experimental study on characterization and properties of eco-friendly nanolubricant containing polyaniline (PANI) nanotubes blended in RBD palm olein oil, J. Therm. Anal. Calorim. 145 (2021) 2967–2981.
[43] A. Afshari, et al., Experimental investigation of rheological behavior of the hybrid nanofluid of MWCNT–alumina/water (80%)–ethylene-glycol (20%) new correlation and margin of deviation, J. Therm. Anal. Calorim. 132 (2018) 1001–1015.
[44] A. Sofiah, et al., Immense impact from small particles: review on stability and thermophysical properties of nanofluids, Sustain. Energy Technol. Assessments 48 (2021), 101635.
[45] M.H. Esfe, et al., Experimental study and sensitivity analysis on the rheological treatment of MWCNT-CuO/SAE50 non-Newtonian hybrid nanofluid to show the usability in industrial applications, Mater. Today Commun. 37 (2023), 107513.
[46] M. Hemmat Esfe, et al., Rheological behavior of 10W40 base oil containing different combinations of MWCNT-Al2O3 nanoparticles and determination of the target nano-lubricant for industrial applications, Micro and Nano Systems Letters 11 (1) (2023) 14.
[47] H. Hatami, et al., Development of knowledge management in investigating the rheological behavior of SiO2/SAE50 nano-lubricant by response surface methodology (RSM), Tribol. Int. 187 (2023), 108667.
[48] S. Sanukrishna, M.J. Prakash, Experimental studies on thermal and rheological behaviour of TiO2-PAG nanolubricant for refrigeration system, Int. J. Refrig. 86 (2018) 356–372.
[49] S. Saedodin, M.H. Kashefi, Z. Bahrami, Experimental study on the rheological behavior of nanolubricant-containing MCM-41 nanoparticles with viscosity measurement, J. Therm. Anal. Calorim. 137 (2019) 1499–1511.
[50] M.H. Esfe, et al., Development of knowledge management for viscosity of nanolubricant in hot and cold lubrication conditions, Tribol. Int. 188 (2023), 108873.

[51] G. Kalpana, K. Madhura, R.B. Kudenatti, Magnetohydrodynamic boundary layer flow of hybrid nanofluid with the thermophoresis and Brownian motion in an irregular channel: a numerical approach, Engineering Science and Technology, an International Journal 32 (2022), 101075.
[52] S. Goudarzi, et al., Nanoparticles migration due to thermophoresis and Brownian motion and its impact on Ag-MgO/Water hybrid nanofluid natural convection, Powder Technol. 375 (2020) 493–503.
[53] M.H. Esfe, et al., Theoretical-Experimental study of factors affecting the thermal conductivity of SWCNT-CuO (25: 75)/water nanofluid and challenging comparison with CuO nanofluids/water, Arab. J. Chem. 16 (5) (2023), 104689.
[54] Y. Guo, et al., A molecular dynamics study on the effect of surfactant adsorption on heat transfer at a solid-liquid interface, Int. J. Heat Mass Tran. 135 (2019) 115–123.
[55] X. Yin, et al., Effects of depositional nanoparticle wettability on explosive boiling heat transfer: a molecular dynamics study, Int. Commun. Heat Mass Tran. 109 (2019), 104390.
[56] Y. Lin, et al., Review on thermal conductivity enhancement, thermal properties and applications of phase change materials in thermal energy storage, Renew. Sustain. Energy Rev. 82 (2018) 2730–2742.
[57] T. Ambreen, M.-H. Kim, Influence of particle size on the effective thermal conductivity of nanofluids: a critical review, Appl. Energy 264 (2020), 114684.
[58] N. Nandhini, S. Rajeshkumar, S. Mythili, The possible mechanism of eco-friendly synthesized nanoparticles on hazardous dyes degradation, Biocatal. Agric. Biotechnol. 19 (2019), 101138.
[59] A.A. Yaqoob, K. Umar, M.N.M. Ibrahim, Silver nanoparticles: various methods of synthesis, size affecting factors and their potential applications–a review, Appl. Nanosci. 10 (2020) 1369–1378.
[60] H. Mercan, Chapter 1 - introduction to nanofluids, challenges, and opportunities, in: M.R. Rahimpour, et al. (Eds.), Nanofluids and Mass Transfer, Elsevier, 2022, pp. 3–20.
[61] B. Bakthavatchalam, et al., Comprehensive study on nanofluid and ionanofluid for heat transfer enhancement: a review on current and future perspective, J. Mol. Liq. 305 (2020), 112787.
[62] B. Mehta, et al., Synthesis, Stability, Thermophysical Properties and Heat Transfer Applications of Nanofluid–A Review, Journal of Molecular Liquids, 2022, 120034.
[63] H. Adun, D. Kavaz, M. Dagbasi, Review of ternary hybrid nanofluid: synthesis, stability, thermophysical properties, heat transfer applications, and environmental effects, J. Clean. Prod. 328 (2021), 129525.